Total Internal Reflection Fluorescence Study of Energy Transfer in Surface-Adsorbed and Dissolved Bovine Serum Albumin†

Thomas P. Burghardt* and Daniel Axelrod

ABSTRACT: A simple adaptation of a commercial spectrofluorometer allows selective excitation of fluorescent biomolecules adsorbed to a solid surface while they are in equilibrium with a bulk solution. As a demonstration of this technique, we have detected a change in the effective singlet–singlet energy transfer in fluorescence-labeled bovine serum albumin (BSA) upon adsorption to a fused silica surface. The technique combines total internal reflection fluorescence excitation of surface-adsorbed BSA with a fluorescence spectroscopic examination of energy transfer between two different fluorophores that are covalently bound to amino groups in each BSA molecule. Two donor–acceptor pairs were used, 4-chloro-7-nitro-2,1,3-benzoxadiazole–rhodamine and dansyl–eosin. For studies of surface-adsorbed BSA, we constructed a device in which the excitation light of a standard fluorescence spectrometer totally internally reflects from a surface at which adsorbed BSA is in equilibrium with the bulk solution. A shallow evanescent wave is created, which excites fluorescence from only those BSA molecules in close proximity to the surface. Spectral examination shows significantly less effective singlet–singlet energy transfer from the donor to the acceptor in surface-adsorbed BSA relative to that in native bulk-dissolved BSA. Under appropriate and reasonable assumptions, the energy transfer change between native and adsorbed states of fluorescent BSA can be interpreted as a conformational change of BSA upon adsorption.

Molecular adsorption at a solid/liquid interface has been under investigation because of its importance in such biological processes as the nonspecific adsorption of serum proteins to a surface (Horbett & Weathersby, 1981; Horbett, 1981; Brash & Lyman, 1971; Watkins & Robertson, 1977; Macritchie, 1978; Kim & Lee, 1979; Neumann et al., 1979) and the complexing of bulk-dissolved ligands to specific receptor molecules immobilized on a surface or imbedded in a cell membrane (Hollenberg & Cuatrecasas, 1978; Mosbach, 1976; Lartique & Yaverbaum, 1976; Ivar, 1978; Weetal, 1972; Adam & Delbrück, 1968; Kronick, 1974). In general, molecular adsorption is a dynamic process that involves adsorption/desorption kinetics and surface diffusion as well as molecular conformation changes.

Surface dynamics of molecules can be studied by total internal reflection fluorescence (TIRF), whereby surface-adsorbed molecules are selectively excited by the evanescent wave of a totally internally reflected light beam. Earlier we measured the adsorption/desorption kinetic rates and surface diffusion coefficient of bovine serum albumin (BSA) adsorbed on fused silica by a technique combining total internal reflection with fluorescence photobleaching recovery (TIR/FPR) (Thompson et al., 1981; Burghardt & Axelrod, 1981). We here adapt TIRF to spectroscopic measurements in a commercial spectrofluorometer equipped with a specially designed sample chamber. In these particular experiments employing this optical system, we examine effective singlet–singlet energy transfer changes in bovine serum albumin upon adsorption to fused silica.

In total internal reflection fluorescence/energy transfer (TIRF/ET), the excitation beam of a fluorescence spectrometer totally internally reflects at a solid/liquid interface, creating an evanescent field that illuminates only those molecules at or very near the surface. This illumination allows the spectroscopic characterization of the surface-bound fluorescence-labeled molecules in chemical equilibrium with the bulk-dissolved ones. Singlet–singlet energy transfer (Förster, 1948) takes place via a dipole–dipole interaction when an excited energy donor is near enough to a suitable energy acceptor to allow transfer of energy from the donor to the acceptor before the donor is deexcited by some other competing process. The efficiency of transfer is highly sensitive to a change in the distance from the donor to the acceptor.

We compare TIRF/ET spectra from adsorbed BSA molecules labeled with fluorescent donors and acceptors to conventional spectra from bulk-dissolved molecules. We observe alterations in the effective energy transfer efficiencies measured from these spectra that in general imply either a conformational change, fluorescence spectral changes, or relative fluorophore orientation changes upon adsorption. If the special assumption of homogeneous spectral properties among the several donors and among the several acceptors on each BSA molecule is valid, then we can further conclude that BSA undergoes a conformational change upon adsorption from a buffer solution to fused silica glass.

Total internal reflection fluorescence spectroscopy (TIRFS), of which TIRF/ET is a particular example, provides a general and convenient means of selectively studying the adsorbed species. With TIRFS, all of the usual fluorescence spectroscopic techniques can be performed on the surface-adsorbed species while it is in chemical equilibrium with the bulk solutions. TIRFS can also be performed on various solid substrates by altering the quartz slide with various surface coatings. Aside from the information obtained about BSA conformational changes, we demonstrate the feasibility of TIRFS as a general technique to study surface chemistry.

Theory

Energy Transfer from a Donor to an Array of Acceptors. A theory of fluorescence energy transfer from a single donor to any array of acceptors has been presented previously (Koppel et al., 1979). Here, we apply their results to our system of several donors and acceptors covalently attached to a large protein molecule with an excess of fluorophore binding

† From the Biophysics Research Division and Department of Physics, University of Michigan, Ann Arbor, Michigan 48109. *Received May 3, 1982; revised manuscript received November 3, 1982.* This work was supported by National Institutes of Health Grants NS14565 and HL24039.

* Address correspondence to this author at the Cardiovascular Research Institute, University of California, San Francisco, San Francisco, CA 94143.

0006-2960/83/0422-0979$01.50/0

sites where the various spatial and orientational distributions of donors and acceptors cannot be readily separated biochemically. First we review the theory for labeled molecules that have a single donor and a particular spatial distribution of acceptors in the donor's vicinity with a particular relative orientation for each donor–acceptor pair. The description is generalized first by ensemble averaging over the range of possible relative orientations for each donor–acceptor pair. We then ensemble average over the different spatial distributions of donors and acceptors that make up an actual sample.

The efficiency of energy transfer, E_{il}, from a single donor to a spatial distribution i of acceptors with a particular set of relative orientations is given by

$$E_{il} = \frac{\Gamma_{il}}{1 + \Gamma_{il}} \tag{1}$$

where

$$\Gamma_{il} = \sum_j [R_{0ij}(l)/R_{ij}]^6 \tag{2}$$

where R_{ij} is the distance from the donor in the ith spatial distribution to the jth acceptor, the sum is taken over all the acceptors j in the spatial distribution i with a particular orientation distribution l between the donor and the acceptors, and $R_{0ij}(l)$ is the donor to acceptor length at which energy transfer is 50% efficient for the jth acceptor. The Förster theory (Förster, 1948) gives

$$R_{0ij}^6(l) = g\epsilon_{A_j}\phi_{D_i}J_{ij}\kappa_{ij}^2(l)n_{ij}^{-4} \tag{3}$$

Here, g is a numerical constant, ϕ_{D_i} is the donor quantum efficiency in the absence of the acceptor, ϵ_{A_j} is the extinction coefficient of the acceptor, J_{ij} is the normalized overlap integral of the donor emission spectrum with the acceptor absorption spectrum, n_{ij} is the refractive index of the medium between the donor and an acceptor, and $\kappa_{ij}(l)$ is the orientation factor for the donor–acceptor pair. In this formalism, additional donors on the molecule are counted simply as members of a different single donor–multiple acceptor spatial distribution i.

Up to this point, eq 1–3 apply to a single protein molecule with one donor and a particular spatial distribution i of acceptors at fixed relative donor–acceptor orientations l. In an actual sample, a whole range of relative orientations, and hence values of R_0, is possible. We average eq 1 over this range of l, thereby defining an ensemble of molecules (denoted the ith ensemble) with donor–acceptor pairs of fixed spatial distribution but varying orientational distribution. This orientational average is denoted by square brackets. We then average over all spatial distributions i, denoted by angular brackets.

$$E_S = \left\langle \left[\frac{\Gamma_{il}}{1 + \Gamma_{il}} \right] \right\rangle \tag{4}$$

Subscript S in E_S denotes the static average. Although the form of eq 4 is generally valid, immobility of fluorophores is implicitly assumed if the averages are taken after the quotient is evaluated.

In the opposite limit of orientational mobility, called the "dynamic limit" (Dale & Eisinger, 1974), the rotational motion is rapid enough so that all the possible relative orientations are sampled many times in the donor excited-state lifetime. When this occurs, $\kappa_{ij}(l)$ is identical for each member in the ith ensemble. Consequently, the orientational average is taken before the quotient is calculated, such that

$$E_D = \left\langle \frac{[\Gamma_{il}]}{1 + [\Gamma_{il}]} \right\rangle \tag{5}$$

Subscript D denotes the dynamic average. In general, the actual energy transfer rate E is always between E_S and E_D such that $E_S \leq E \leq E_D$.

An approximation to E_S and E_D can be written as

$$E_L = \frac{\langle [\Gamma_{il}] \rangle}{1 + \langle [\Gamma_{il}] \rangle} \tag{6}$$

Note that, in general, $E_D \leq E_L$. E_L is a good approximation to E_S and E_D only if E is small (Dale et al., 1979). For this reason, the subscript L denotes a low energy transfer efficiency limit.

The difficult question in practice is how small E must be, given a particular spatial and orientational distribution, to ensure the system is in the low energy transfer efficiency limit. Using a reasonable spatial and orientational distribution for our protein system, we show in the Appendix the conditions under which eq 6 is an appropriate estimate of E.

Energy Transfer Spectroscopic Measurements. We now introduce the special assumption that the extinction coefficients and quantum efficiencies (in the absence of energy transfer) do not vary from donor to donor and acceptor to acceptor, i.e., that $\epsilon_{D_i} = \epsilon_D$, $\phi_{D_i} = \phi_D$, $\epsilon_{A_j} = \epsilon_A$, $\phi_{A_j} = \phi_A$, $J_{ij} = J$, and $n_{ij} = n$. From spectra of the donor–acceptor system, we can measure the quantities F_A and F_D, the fluorescence intensities experimentally observed at a fixed acceptor and donor emission wavelength, respectively, for excitation at a fixed donor excitation wavelength, such that

$$F_A = N\epsilon_D\phi_A f_A E C_D \tag{7}$$

$$F_D = N\epsilon_D\phi_D f_D(1 - E)C_D \tag{8}$$

where N is a numerical constant depending on the light collection efficiency of the fluorescence spectrometer, ϵ_D is the extinction coefficient of the donor, $\phi_{A(D)}$ is the quantum efficiency of the acceptor (donor), C_D is the donor concentration, and $f_{A(D)}$ is the shape function, normalized with unity area, of the acceptor (donor) emission spectrum. From eq 7 and 8, we obtain

$$\frac{E}{1 - E} = \frac{F_A}{F_D}\frac{\phi_D f_D}{\phi_A f_A} \tag{9}$$

For a system in the low energy transfer efficiency limit, we combine eq 9 with eq 6 to find

$$\langle [\sum_j \kappa_{ij}^2(l)/R_{ij}^6] \rangle = \frac{F_A}{F_D}\frac{f_D n^4}{gJ\epsilon_A f_A \phi_A} \tag{10}$$

Comparing eq 10 for bulk-dissolved vs. surface-adsorbed molecules, we can form the intramolecular distance and orientation ratio, χ, such that

$$\chi \equiv \frac{\langle [\sum_j \kappa_{ij}^2(l)/R_{ij}^6] \rangle}{\langle [\sum_j \kappa_{ij}'^2(l)/R_{ij}'^6] \rangle} = \frac{F_A}{F_D}\frac{F'_D}{F'_A}\frac{J'\epsilon'_A f'_A \phi'_A f_D n^4}{J\epsilon_A f_A \phi_A f'_D n'^4} \tag{11}$$

where the unprimed and primed variables stand for the bulk-dissolved and surface-adsorbed species, respectively. The experiments discussed here were performed to detect a conformational change from the bulk-dissolved to the surface-adsorbed species. A value of the right side of eq 11 not equal to unity implies a conformational change upon adsorption (under the assumption of spectroscopic homogeneity discussed earlier). The conformational change can be further interpreted as a change in the intermolecular donor–acceptor separation distance if the orientational factors, $\kappa_{ij}^2(l)$, are not altered by adsorption.

Application of eq 11 requires low energy transfer efficiency. Determination of the quantum efficiency using fluorescence

lifetime measurements would allow E to be calculated directly from eq 9. Lifetime measurements can be done directly on the surface-adsorbed species by using TIRFS in a fluorescence lifetime spectrofluorometer. Without the fluorescence lifetime measuring capability, E can be obtained indirectly by using eq 9 and the relation

$$\mathcal{F}_{A(D)} \propto A_{A(D)}\phi_{A(D)}f_{A(D)} \tag{12}$$

where $\mathcal{F}_{A(D)}$ is the acceptor (donor) fluorescence in the absence of the donor (acceptor) and $A_{A(D)}$ is the absorption coefficient of the acceptor (donor) to obtain

$$E = \frac{1}{1 + (F_D/F_A)(\mathcal{F}_A/\mathcal{F}_D)(A_D/A_A)} \tag{13}$$

The ratio of the absorption coefficient of the donor to that of the acceptor can be measured by using a conventional absorption spectrometer. For the surface-adsorbed BSA, the optical densities are very low but can still be measured by using a special multiple sample chamber described elsewhere (Burghardt & Axelrod, 1981). Because of inaccuracies that result when these low optical densities are measured, the precision of the results for E (bulk) and E' (adsorbed) from eq 13 is somewhat lower than those for χ from eq 11. For this reason, we present our main results as the ratio χ.

Materials and Methods

Total Internal Reflection Fluorescence Spectroscopy. Total internal reflection of a light beam incident on an interface from a medium of higher refractive index (e.g., quartz glass) to one of lower refractive index (e.g., aqueous solution) occurs if the incidence angle is greater than the critical angle, $\theta_c = \sin^{-1}(n_2/n_1)$, with n_2 and n_1 referring to lower and higher refractive indices, respectively. The incident light creates an evanescent field in the lower refractive index medium with an intensity that exponentially decays with distance from the interface with a characteristic depth of a fraction of a wavelength of the incident light (Harrick, 1967). In our experiments, fluorescent-labeled BSA molecules adsorb in equilibrium at a quartz glass/aqueous buffer interface. Only the fluorescent-labeled molecules within the evanescent field become excited and fluoresce. In general, some nonadsorbed fluorescent molecules in the bulk solution within the depth of the evanescent field may be excited. However, this contribution to the total fluorescence is negligible in our experiments (Burghardt & Axelrod, 1981; Appendix A): almost all of the fluorescence originates from BSA adsorbed to the surface.

The total internal reflection device we have constructed, shown in Figure 1, consists of a quartz hemicylinder in optical contact with a square quartz microscope slide. The quartz slide is in contact with a bulk solution reservoir made from a Plexiglass hemicylindrical shell of the same outside diameter as the prism. The reservoir is sealed at the bottom, and the quartz slide in contact with the Plexiglass shell is made water tight with silicone grease. The prism and slide and reservoir unit (the TIRFS device) is mounted on a base that allows the device to rotate. The base is mounted for easy removal in an x-y translator for lateral positioning of the device that fits in the cuvette chamber of a commercial fluorescence spectrometer with the standard cuvette holder removed. Incident light from the excitation monochromator travels through the prism and contacting slide and strikes the quartz/water interface at an angle of incidence of 80°. This is greater than the critical angle of 65.4° for a quartz/water interface, and the light therefore totally internally reflects. The TIRFS device is positioned laterally so that the fluorescent emission originating from the evanescent field region passes back through the slide and prism

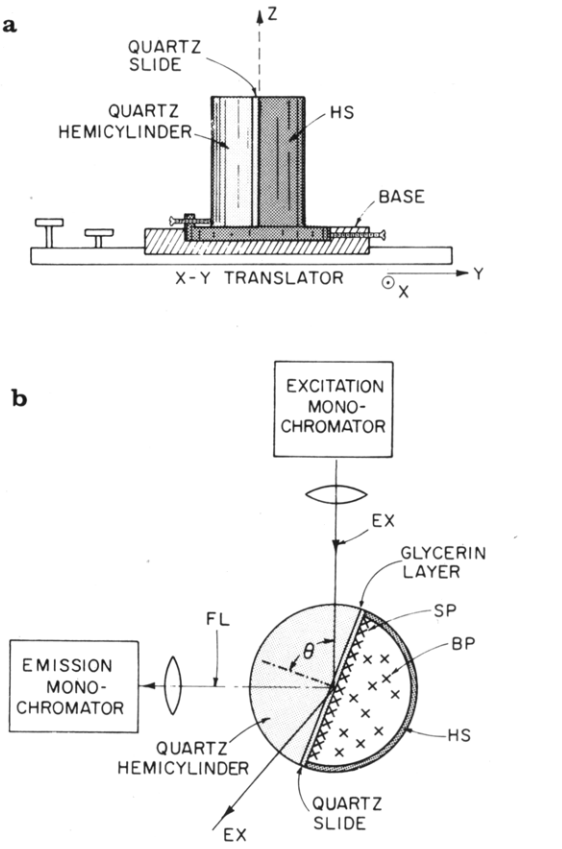

FIGURE 1: Two views of the total internal reflection fluorescence spectroscopy (TIRFS) apparatus. (a) Side view shows the axis of rotation, z, about which the prism and slide and Plexiglass hemicylinder shell (HS) unit is rotated in the base to adjust the angle of incidence of the excitation light. The base is removably mounted on an x-y translator for lateral positioning of the unit. The apparatus fits inside the sample chamber of a commercial fluorescence spectrofluorometer. (b) Vertical view of the device shows the path of the excitation (EX) and the fluorescent emission (FL) through the quartz hemicylinder. Surface-adsorbed protein (SP) is illuminated by the evanescent field while in chemical equilibrium with the bulk-dissolved protein (BP). The angle of incidence of the excitation light, θ, in the experiments reported here was 80°; the critical angle is $\theta_c = 65.4°$ for this system. The fused quartz hemicylinder (Harrick Scientific) has a radius of 1.3 cm and a height of 2.5 cm.

toward the emission monochromator; this design avoids any absorption of the emitted light by the bulk solution. With TIRFS, all of the usual spectroscopic measurements can be performed on a surface-adsorbed layer while it is in chemical equilibrium with the bulk solution.

TIRFS spectra were obtained ~1 h after labeled BSA was placed in the reservoir to allow the adsorption to reach quasi-equilibrium. Spectra of bulk dissolved BSA were taken with the sample in a conventional 1-cm^2 rectangular quartz cuvette. All spectra, whether conventional or TIRF, were taken on a SLM 4000 spectrofluorometer (SLM Instruments, Inc.; Urbana, IL) operated in the excitation correction mode. For some experiments, polarized TIRF spectra were taken simply by placing Glan-Thompson polarizers in the excitation and emission beam.

Preparation of Dansyl–Eosin–BSA and NBD–Rhodamine–BSA and the Glass Surface. The BSA molecules were covalently labeled with the fluorescent donor–acceptor pairs dansyl–eosin (D–E–BSA) and NBD–tetramethylrhodamine (N–R–BSA). They are compatible for energy transfer because their spectral overlap, J, is favorable and the separation of their emission spectra allows acceptor and donor emissions to be easily distinguished.

Twenty-five milligrams of crystallized BSA (Sigma Chemical Co.; St. Louis, MO; essentially fatty acid free) was dissolved in 2.5 mL of 0.1 M sodium bicarbonate buffer, pH 9.0. An excess of eosin 5-isothiocyanate powder (Molecular Probes, Inc., Junction City, OR) was added and allowed to react with the BSA for ~1 min with continuous stirring. The reaction mixture was then passed through a column of Sephadex G-50 made in 5 mM sodium phosphate plus 150 mM NaCl buffer, pH 7.0 (PBS), to separate excess unreacted eosin from labeled protein. Typically, this procedure yielded 5–10 eosin groups per protein molecule.

Dansyl chloride (Molecular Probes) was dissolved in isopropyl alcohol at a concentration of 10 mg/mL. The dansyl in alcohol was added stoichiometrically (five dansyl groups per protein molecule) to the eosin–BSA dissolved in PBS and allowed to react for ~5 min with continuous stirring. The solution was then passed through another column of Sephadex G-50 made in PBS to remove unreacted dansyl groups. The doubly labeled protein was dialyzed in PBS for ~24 h to remove any remaining fluorophore groups that may have nonspecifically attached to the BSA.

Preparation of N–R–BSA is analogous to the above where tetramethylrhodamine isothiocyanate (Research Organics, Inc.; Cleveland, OH) is handled like eosin and 4-chloro-7-nitro-2,1,3-benzoxadiazole (NBD) (Molecular Probes) like dansyl except that NBD is added as a powder to the R–BSA solution. The preparation of the slides was identical with that described elsewhere (Burghardt & Axelrod, 1981).

Results

The goal of the spectroscopic measurements is to calculate χ by using eq 11. The right side of eq 11 contains two ratios that involve the spectral change in the fluorescent probes due to surface adsorption of the protein molecule to which they are attached. The first is the ratio of the spectral overlap integrals. Overlap integrals are calculated from the normalized fluorescence emission spectrum of the donor without the acceptor present and the normalized excitation spectrum of the acceptor without the donor present, for both the bulk-dissolved (J) found under conventional illumination and the surface-adsorbed (J') found under TIRFS. Although we found the shapes of the spectra to be virtually unchanged by adsorption, there was a small shift in the maxima that caused a larger overlap in the adsorbed species. We found $J'/J = 1.25 \pm 0.05$ for both types of labeled BSA molecules.

The other ratio in eq 11 compares the fluorescence emission intensity of acceptors bound to surface-adsorbed BSA to the same total number of acceptors bound to bulk-dissolved BSA molecules. To be sure that fluorescence intensities from equal numbers of acceptors in the two states are compared, we devised a depletion method to measure the acceptor surface concentration of adsorbed BSA. Finely ground quartz glass was added to a known amount of bulk-dissolved acceptor-labeled BSA (A–BSA) that adsorbs to the particles. We vigorously washed the quartz particles twice to remove any reversibly bound A–BSA. The quartz particles were then separated from the liquid fraction by centrifugation, and the fluorescent emission intensity and spectrum of the liquid fraction were compared to those of a standard A–BSA bulk concentration. This procedure allowed determination of the amount of A–BSA left on the quartz particles. The particles were then resuspended in buffer in a spectrofluorometer rectangular cuvette, and the acceptor emission intensity and spectrum of surface-adsorbed A–BSA were thereby obtained by conventional fluorescence excitation and 90° emission. The adsorbed BSA intensity and spectrum were then compared directly to those of the same concentration of bulk-dissolved A–BSA. These experiments indicate there is a shape change in the emission spectrum of eosin for surface-bound E–BSA compared to bulk-dissolved E–BSA; there is no observed change in the emission spectrum of rhodamine in R–BSA. The correction for the spectral change of surface-adsorbed E–BSA depends on the wavelength observed and is included in our results.

Table I: Intramolecular Distance and Orientation Ratio (χ) for One Experiment Using Dansyl–Eosin–BSA and for Three Different Experiments with NBD–Rhodamine–BSA[a]

D–E–BSA	N–R–BSA
1.4 ± 0.3	1.6 ± 0.2
	2.0 ± 0.2
	3.2 ± 0.2

[a] The total uncertainty in χ includes estimated experimental uncertainties and the estimated error introduced by the use of the low energy transfer efficiency limit approximation as described in the Appendix.

To finally determine χ, the intramolecular distance and orientation ratio as derived in eq 11, we measured the fluorescence spectra for the bulk-dissolved and surface-adsorbed D–E–BSA and N–R–BSA. The values of F_A, F'_A, F_D, and F'_D are measured from the excitation and emission spectra; applicable spectra for N–R–BSA are shown in Figure 2. On the basis of these experimental results and also with the assumption that $n = n'$, the values of χ for N–R–BSA and D–E–BSA are calculated and summarized in Table I. Under the stated assumptions, the results that $\chi > 1$ indicates that D–E–BSA and N–R–BSA undergo a conformational change upon adsorption to fused silica. Under the further assumption that relative donor–acceptor orientation is not significantly altered by adsorption, the experimental results that $\chi > 1$ indicate a spreading of the BSA conformation upon adsorption to fused silica.

Our calculation of χ using eq 11 assumes both the surface-adsorbed and bulk-dissolved systems are in the low energy transfer efficiency limit. The error introduced by this approximation is calculated in the Appendix and is included in the total uncertainty for each experimental value of χ in Table I.

Effective energy transfer efficiencies (E and E') were calculated from experimental measurements via eq 13. In a typical N–R–BSA preparation, $E = 0.008$ and $E' = 0.003$; for a typical D–E–BSA preparation, $E = 0.14$ and $E' = 0.12$. Clearly, the transfer of donor energy to the array of acceptors is not a likely event in either of these systems, and the transfer efficiency tends to decrease upon adsorption.

Discussion

The experiments reported here demonstrate the adaptability of total internal reflection optics to a commercial spectrofluorometer for the study of biomolecular interactions at a surface. The particular application to singlet–singlet energy transfer here revealed a decrease of effective energy transfer efficiency in multiple-labeled BSA upon surface adsorption.

Various assumptions were employed to allow interpretation of the transfer efficiency change in terms of a protein conformational change. First, we assumed that all of the donors and all of the acceptors are spectroscopically equivalent. Nonetheless, it is possible that the extinction coefficients and quantum efficiencies vary according to the immediate local environment of each fluorophore. In calculating the intramolecular distance and orientation ratio χ, we have accounted for small changes in the *average* spectral features of donors

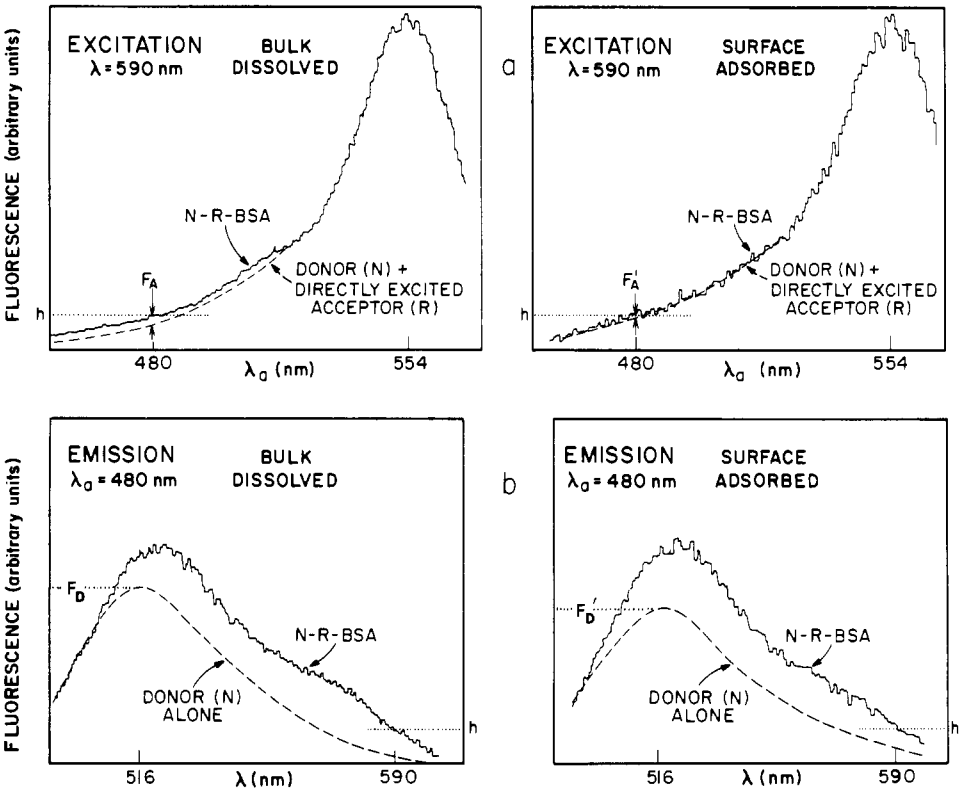

FIGURE 2: (a) Excitation and (b) emission spectra for bulk-dissolved and surface-adsorbed N–R–BSA. The solid curves are spectra of BSA labeled with both donors (NBD) and acceptors (rhodamine). The dashed curves in (a), derived from actual spectra of BSA labeled with donors alone (N–BSA) and with acceptors alone (R–BSA), represent the portion of the N–R–BSA excitation spectra due to direct donor emission plus direct acceptor emission. The dashed curves in (b) represent the portion of the total emission of N–R–BSA due to the emission of only the donor in N–R–BSA. The excitation and emission spectra are normalized so that the measured fluorescence intensities (h) at excitation wavelength λ = 480 nm and emission wavelength λ = 590 are equal. The quantities F_A, F_D, F'_A, and F'_D as used in eq 11 are also shown. The four panels are actual runs showing the signal/noise ratio one can expect from single spectral scans. The bulk concentration of N–R–BSA and spectra scan speeds were, respectively, 0.1 mg/mL and 1 s/nm for conventional bulk-dissolved experiments and 1 mg/mL and 10 s/nm for surface-adsorbed TIRF experiments.

and acceptors due directly to adsorption to fused silica glass. The theory, experimental protocols, and interpretation presented here should apply exactly to biochemical systems containing a single donor and acceptor in identical positions on all molecules.

A second assumption involved setting the intramolecular index of refraction n for bulk-dissolved BSA equal to the index of refraction n' for surface-adsorbed BSA. (Again, a uniform average for each is assumed.) Index n' could conceivably be closer to that of fused silica (1.467) and n closer to that of water (1.333). However, these are extreme values, and both n and n' are likely to be considerably closer in value, determined at least partially by the intramolecular polarizability of the protein itself.

A third assumption involves the use of the low energy transfer limit form (eq 6) to derive the form for χ (eq 11). The Appendix calculates the maximum error this assumption might introduce, but the calculation itself depends on a specific model of an orientational and spatial distribution of donors and acceptors. The chosen model is physically very reasonable, but more pathological and unrealistic models do exist in which eq 6 would not be as good an approximation.

Two special properties of TIRF/ET require attention when the fluorescence spectra are interpreted. First, the evanescent field intensity is dependent on the wavelength of the excitation light. We have calculated the evanescent field intensity (Harrick, 1967) by using published values for the refractive indices of water and quartz (Holloway, 1973; Dorsey, 1940). At the wavelengths used here, the evanescent field intensity is ~9% brighter at the excitation peak of the donor compared to the acceptor. This effect would cause the donor excitation peak to be relatively more prominent in TIRF/ET than in bulk spectra. Since we actually observe the opposite effect, our interpretation of the spectral change as representing decreased energy transfer efficiency upon adsorption is only strengthened. Second, the close association and higher concentration of fluorophores on the surface because of adsorption may increase the energy transfer efficiency by increasing the probability of transfer between different BSA molecules. Since we observe a decreased energy transfer efficiency upon adsorption, the high surface concentration effect again favors our interpretation of the data.

Measurement of the surface-adsorbed concentration (to deduce extinction coefficient and quantum efficiency changes upon adsorption) is required to accurately interpret TIRF/ET results. The use of the quartz particles, described under Results, accomplished this purpose. The quartz particles could theoretically have been used in place of total internal reflection. This would be awkward from an experimental standpoint because the particles cause artifacts from excitation light scattering and the gradual settling of the particles from solution. These problems can be overcome, and we did so, but they make experiments difficult to perform and hence prone to error. The combination of TIRFS with the quartz particles as described here reduces the use of the particles to one simple experiment. There is also a significant difference in what the two techniques actually measure. TIRFS observes all the surface-bound molecules in equilibrium with the bulk-dissolved ones, i.e., both irreversibly and reversibly bound molecules. The quartz particle method observes only irreversibly bound

molecules. Other possible methods of surface calibration may circumvent the quartz particles method (Burghardt, 1982).

TIRFS can easily be set up in a conventional fluorescence spectrometer and used to study spectroscopic properties of a surface-bound molecule. With TIRFS, spectroscopic properties of the adsorbed molecules are measured while they are in chemical equilibrium with the bulk-dissolved molecules. An intrinsic spectroscopic difference between the bound and unbound molecules is not required. We have demonstrated the usefulness of TIRFS in the form of TIRF/ET in detecting conformational change upon nonspecific adsorption. The technique (TIRFS) can be extended to other systems (e.g., spectroscopic changes in specific binding such as ligand–membrane receptor binding) and to other fluorescence techniques [e.g., intrinsic protein fluorescence (Van Wagenen et al., 1981), fluorescence polarization (T. P. Burghardt, unpublished experiments), and time-resolved fluorescence techniques]. Apart from its inherent usefulness, TIRFS compliments TIR/FPR and TIR/FCS (Thompson et al., 1981; Burghardt & Axelrod, 1981) in the characterization of molecular dynamics at a solid/liquid interface.

Acknowledgments

We acknowledge Dr. Nancy L. Thompson for her help in designing and building the TIRFS device and for her critical reading of the manuscript. We thank Debbie Rapley for typing the manuscript.

Appendix

The experimental results for ratio χ reported in Table I were computed by assuming the system is in the low energy transfer efficiency limit. In this limit, we need not explicitly assume any particular spatial or orientational distribution of fluorophores or rates of rotational motion. A correct calculation for the "true" χ ratio for a system residing somewhere in between the static and dynamic limits does depend on these unknowns. How much might we expect the experimental χ to deviate from the true χ? To calculate an approximate answer, we will calculate a theoretical χ, χ_{th}, in a situation for which we assume an explicit form for spatial and orientational distributions. We adopt a model in which the protein molecule is described by a spheroidal surface with acceptors distributed at random over the surface. For this calculation, we also assume that all of the donor–acceptor pairs have isotropically distributed orientations. Koppel et al. (1979) have derived the energy transfer efficiency for this system. From their equations, it is easy to show that E_S and E_D are approximated by

$$E_S = \sigma \int_{W_0}^{W} dW_1 \left[\frac{\Gamma_{il}}{1 + \Gamma_{il}} \right] \exp[-\sigma(W_1 - W_0)] \quad \text{(A1)}$$

$$E_D = \sigma \int_{W_0}^{W} dW_1 \frac{[\Gamma_{il}]}{1 + [\Gamma_{il}]} \exp[-\sigma(W_1 - W_0)] \quad \text{(A2)}$$

where σ is the surface density of acceptors on the protein, the square brackets denote an isotropic dipole orientation average (Dale et al., 1979), W is the total surface area of the protein, and W_0 is an area surrounding each donor from which the nearest acceptor is excluded. E_L is calculated by using eq 6 and

$$\langle [\Gamma_{il}] \rangle = \int_{W_0}^{W} dW_1 [\Gamma_{il}] \exp[-\sigma(W_1 - W_0)] \quad \text{(A3)}$$

The explicit dependence of $[\Gamma_{il}]$ on W_1 is given elsewhere (Koppel et al., 1979). Values for E_D and E_L were tabulated numerically as a function of $\langle [R_0] \rangle$, given W as found in the literature (Peters & Reed, 1977) and σ as determined experimentally to be between 5 and 10 acceptors per protein molecule.

Since ultimately we wish to test the significance of our experimental results of $\chi > 1$, we will calculate χ_{th} by assuming that the decrease in effective energy transfer efficiency upon adsorption is due not to a BSA conformational change but instead entirely to a difference in fluorophore rotation rates between bulk and surface-adsorbed BSA. The maximal decrease in energy transfer upon adsorption would occur if the rotations were dynamically averaged in the bulk and statistically averaged on the surface. Using the definition of χ in eq 11 derived from the low energy transfer limit and using eq 2 and 3, we can write

$$\chi_{th} = \frac{Q'}{Q} \frac{E_L/(1 - E_L)}{E'_L/(1 - E'_L)} \quad \text{(A4)}$$

where Q' and Q are numerical and spectroscopic constants for adsorbed and bulk BSA, respectively. E_L is calculated as follows. The experimentally observed E (from eq 13) is set equal to E_D of eq A2, from which an appropriate $\langle [R_0] \rangle$ value is calculated (given the reasonable assumptions of $\sigma = 5$ and $W_0 = 1257$ Å^2, corresponding to a closest approach of donor and acceptor of 20 Å). This $\langle [R_0] \rangle$ value (which turns out to be $\approx$18 Å) is then used to determine E_L, via eq A3. E'_L is calculated analogously, except for starting with the experimentally observed E' set equal to E_S of eq A1. The error $(\chi - \chi_{th}/\chi$ is then combined with measurement uncertainties to obtain the total uncertainty in each χ value quoted in Table I.

References

Adam, G., & Delbrück, M. (1968) in *Structural Chemistry and Molecular Biology* (Rich, A., & Davidson, N., Eds.) W. H. Freeman, San Francisco, CA.

Brash, J. L., & Lyman, D. J. (1971) in *The Chemistry of Biosurfaces* (Hair, M., Ed.) p 177, Marcel Dekker, New York.

Burghardt, T. P. (1982) Ph.D. Thesis, University of Michigan, Ann Arbor, MI.

Burghardt, T. P., & Axelrod, D. (1981) *Biophys. J. 33*, 455.

Dale, R. E., & Eisinger, J. (1974) *Biopolymers 13*, 1573.

Dale, R. E., Eisinger, J., & Blumberg, W. (1979) *Biophys. J. 26*, 161.

Dorsey, N. E. (1940) *Properties of Ordinary Water-Substance*, Reinhold, New York.

Förster, T. (1948) *Ann. Phys. (Leipzig) 2*, 55.

Harrick, N. J. (1967) *Internal Reflection Spectroscopy*, Wiley, New York.

Hollenberg, M. D., & Cuatrecasas, M. D. (1978) *Prog. Neuro-Psychopharmacol. 2*, 287.

Holloway, D. G. (1973) *The Physical Properties of Glass*, Wykeham Publications, London.

Horbett, T. A. (1981) *J. Biomed. Mater. Res. 15*, 673.

Horbett, T. A., & Weathersby, P. K. (1981) *J. Biomed. Mater. Res. 15*, 403.

Ivar, G. (1978) *J. Immunol. Methods 24*, 57.

Kim, S. W., & Lee, E. S. (1979) *J. Polym. Sci., Polym. Symp. No. 66*, 429.

Koppel, D. E., Fleming, P. J., & Strittmater, P. (1979) *Biochemistry 18*, 5450.

Kronick, M. (1974) Ph.D. Thesis, Stanford University, Stanford, CA.

Lartique, D. J., & Yaverbaum, S. (1976) in *Progress in Surface and Membrane Science* (Cadenhead, D. A., & Danielli, J. F., Eds.) p 361, Academic Press, New York.

Macritchie, F. (1978) *Adv. Protein Chem. 32*, 283.
Mosbach, K. (1976) *Methods Enzymol. 44*.
Neumann, A. W., Moscarello, M. A., Zingg, W., Hum, O. S., & Chang, S. K. (1979) *J. Polym. Sci., Polym. Symp. No. 66*, 391.
Peters, T., & Reed, R. G. (1977) *FEBS Lett. 50*, 11.
Thompson, N. L., Burghardt, T. P., & Axelrod, D. (1981) *Biophys. J. 33*, 435.
Van Wagenen, R., Rockhold, S., & Andrade, J. (1982) *Biomaterials: Interfacial Phenomena and Applications* (Cooper, S., & Peppas, N., Eds.) Adv. Chem. Ser. No. 199, p 351, American Chemical Society, Washington, DC.
Watkins, R. W., & Robertson, C. R. (1977) *J. Biomed. Mater. Res. 11*, 915.
Weetal, H. H. (1972) in *The Chemistry of Biosurfaces* (Hair, M. L., Ed.) p 597, Marcel Dekker, New York.

Role of Calmodulin in Skeletal Muscle Sarcoplasmic Reticulum†

Michele Chiesi and Ernesto Carafoli*

ABSTRACT: Three proteins having M_r of 20 000, 35 000, and 57 000 were phosphorylated by a calmodulin-dependent system in fast skeletal muscle sarcoplasmic reticulum (SR). The 20 000-dalton phosphoprotein was an acidic proteolipid distinct from phospholamban, which was present in cardiac SR preparations. The 57 000-dalton phosphoprotein became phosphorylated very rapidly ($t_{1/2}$ = 5–10 s at 0 °C) and was distinct from calsequestrin and the 53 000-dalton glycoprotein, as judged from the electrophoretic mobility on neutral Laemmli gels and from its detergent-extraction characteristics. None of the three phosphoproteins interacted directly with calmodulin, implying that they were not the regulatory subunit of the calmodulin-dependent kinase. The calmodulin-dependent kinase(s) responsible for the phosphorylation of the three protein substrates was (were) membrane bound. Its K_m(ATP) was about 200 μM, and at the probable physiological calmodulin concentration of 1–2 μM, its K_m(Ca) was 0.7 μM. The 57 000-dalton phosphoprotein was dephosphorylated by an endogenous phosphatase activity, which was also activated by the Ca–calmodulin complex.

The role of calmodulin in heart sarcoplasmic reticulum (SR) has been intensively investigated in the last 3 or 4 years. A stimulation of Ca^{2+} transport in cardiac SR vesicles was first reported by Katz & Remtulla (1978) and soon confirmed in several other laboratories (LePeuch et al., 1979; Wuytack et al., 1980; Bilezikjian et al., 1980). As a result of these studies, a complex calmodulin-dependent system for the regulation of the cardiac SR Ca^{2+} pump has now come to light. It apparently operates in parallel with the regulatory system, which depends on cAMP and a specific kinase and which phosphorylates the hydrophobic intrinsic protein phospholamban (Tada et al., 1975; Wray & Gray, 1977). The calmodulin-dependent system requires Ca^{2+}, is mediated by a specific kinase (LePeuch et al., 1979), and also phosphorylates phospholamban. The sites of phospholamban phosphorylation by the two systems are apparently different (LePeuch et al., 1979). Direct evidence for the existence of a calmodulin-dependent protein kinase in heart SR has recently been provided by Jones & Wegener (1981). A protein fraction containing kinase activity was separated from detergent-solubilized heart SR by calmodulin affinity chromatography and shown to phosphorylate more than one protein in the SR membrane.

Calmodulin is now known to be present in SR different from heart (Carafoli et al., 1980), including skeletal muscle. Two detailed studies on the latter tissue have recently appeared (Chiesi & Carafoli, 1982; Campbell & MacLennan, 1982). In one (Campbell & MacLennan, 1982), calmodulin was shown to mediate the phosphorylation of two SR proteins, a major one having M_r of 60 000 and a minor one of M_r 20 000. The suggestion was made that the calmodulin-dependent phophorylation may mediate the release of Ca^{2+} from SR vesicles. In the other (Chiesi & Carafoli, 1982), calmodulin was found to promote the phosphorylation of three SR proteins, having M_r of 57 000, 35 000, and 20 000. Also in this study, the conclusion was reached that the phosphorylation of these three proteins has no influence on the active Ca^{2+} uptake but may regulate its release from the vesicles.

The purpose of the present work has been the systematic study of the calmodulin-dependent phosphorylation of proteins in the various cell fractions leading to the final isolation of purified skeletal muscle SR membranes and the characterization of those unequivocally attributable to the SR membrane in terms of their possible role in the calmodulin regulation system. The results have corroborated the previous conclusion that skeletal muscle membranes contain three proteins that are substrates of the calmodulin-promoted phosphorylation. Those having M_r of 57 000 and 20 000 appear to be the major substrates. None of the three proteins, however, interacts directly with calmodulin; i.e., they are not identical with the calmodulin-dependent kinase nor with its regulatory subunit. The study has shown that, in addition to the specific calmodulin-dependent kinase, skeletal muscle SR membranes also contain a calmodulin- (plus Ca^{2+}) dependent phosphatase. The phosphorylated M_r 57 000 protein is one of its substrates.

Materials and Methods

Hexokinase (type VII) and cAMP-dependent protein kinase from rabbit muscle were obtained from Sigma. [γ-^{32}P]ATP (2–10 Ci/mmol) was obtained from New England Nuclear. Calmodulin was isolated from bovine brain according to Watterson et al. (1976). Azidocalmodulin was prepared as described (Andreasen et al., 1981). Calmodulin was conjugated to CNBr-activated Sepharose 4B (Pharmacia) as previously described (Niggli et al., 1979). SR was isolated from rabbit white muscles according to Eletr & Inesi (1972).

† From the Laboratory of Biochemistry, Swiss Federal Institute of Technology (ETH), 8092 Zürich, Switzerland. *Received August 27, 1982.* The financial contribution of the Swiss Nationalfonds (Grant No. 3.634-0.80) is gratefully acknowledged.

0006-2960/83/0422-0985$01.50/0